Journal of Zhejiang University-SCIENCE B (Biomedicine & Biotechnology)
ISSN 1673-1581 (Print); ISSN 1862-1783 (Online)
www.zju.edu.cn/jzus; www.springerlink.com
E-mail: jzus@zju.edu.cn

Involvement of phosphatidate phosphatase in the biosynthesis of triacylglycerols in *Chlamydomonas reinhardtii*[*#]

Xiao-dong DENG[1], Jia-jia CAI[1], Xiao-wen FEI[†‡2]

([1]*Key Laboratory of Tropical Crop Biotechnology, Ministry of Agriculture, Institute of Tropical Bioscience and Biotechnology, Chinese Academy of Tropical Agricultural Sciences, Haikou 571101, China*)

([2]*School of Science, Hainan Medical College, Haikou 571101, China*)

[†]E-mail: Feixw2000@hotmail.com

Received July 2, 2013; Revision accepted Oct. 18, 2013; Crosschecked Nov. 7, 2013

Abstract: Lipid biosynthesis is essential for eukaryotic cells, but the mechanisms of the process in microalgae remain poorly understood. Phosphatidic acid phosphohydrolase or 3-*sn*-phosphatidate phosphohydrolase (PAP) catalyzes the dephosphorylation of phosphatidic acid to form diacylglycerols and inorganic orthophosphates. This reaction is integral in the synthesis of triacylglycerols. In this study, the mRNA level of the PAP isoform *CrPAP2* in a species of *Chlamydomonas* was found to increase in nitrogen-free conditions. Silencing of the *CrPAP2* gene using RNA interference resulted in the decline of lipid content by 2.4%–17.4%. By contrast, over-expression of the *CrPAP2* gene resulted in an increase in lipid content by 7.5%–21.8%. These observations indicate that regulation of the *CrPAP2* gene can control the lipid content of the algal cells. In vitro CrPAP2 enzyme activity assay indicated that the cloned *CrPAP2* gene exhibited biological activities.

Key words: Phosphatidate phosphohydrolase 2, Triacylglycerol biosynthesis, RNAi, *Chlamydomonas reinhardtii*, Nitrogen deprivation, Over-expression

doi:10.1631/jzus.B1300180 **Document code:** A **CLC number:** Q291

1 Introduction

With rapidly decreasing fossil fuel resources, the importance of energy and environmental preservation has received increasing interest. Microalgae biodiesel, a crucial part of renewable biomass energy that uses solar energy to convert CO_2 into biomass, is the most promising alternative for fossil fuels. However, the study of lipid metabolism in the eukaryotic single-celled photosynthetic microalgae has lagged behind that of oil crops. Basic knowledge of microalgae has long fallen behind that of most crops, such as rice, rape, and corn. However, with the increasing number of microalgae-derived biodiesel studies on a global scale, more research teams are focusing on the underlying mechanisms of high lipid production and high cell density cultures. These processes are crucial to the improvement of genetic strains, and to the future cultivation of commercial and industrial microalgae. Phosphatidic acid phosphohydrolase (3-*sn*-phosphatidate phosphohydrolase, PAP, EC 3.1.3.4) catalyzes the dephosphorylation of phosphatidic acid to form diacylglycerols and inorganic

‡ Corresponding author

* Project supported by the National Natural Science Foundation of China (Nos. 30960032 and 31000117), the Major Technology Project of Hainan (No. ZDZX2013023-1), the National Nonprofit Institute Research Grants (Nos. CATAS-ITBB110507 and CATAS-ITBB 130305), the Fundamental Scientific Research Funds for Chinese Academy of Tropical Agricultural Sciences (No. 1630052013009), and the Natural Science Foundation of Hainan Province (No. 313077), China

Electronic supplementary materials: The online version of this article (doi:10.1631/jzus.B1300180) contains supplementary materials, which are available to authorized users

orthophosphates (Smith *et al*., 1957). Depending on their requirement for Mg^{2+}, PAPs are classified as either Mg^{2+}-dependent or Mg^{2+}-independent. An Mg^{2+}-dependent PAP is referred to as *PAP1*, whereas an Mg^{2+}-independent PAP is generally referred to as lipid phosphate phosphatase (LPP) or *PAP2*. PAPs are involved in lipid biosynthesis or lipid signaling (Carman, 1997; Sciorra and Morris, 2002; Nanjundan and Possmayer, 2003). In mammalian cells, *PAP2* reportedly participates in lipid signal transduction (Brindley, 2004), but the function of *PAP1* remains unknown.

In eukaryotic cells, triacylglycerol (TAG) biosynthesis is important. This process starts from glycerol-3-phosphate and Acyl-coenzyme A to form lysophosphatidic acid. This reaction is catalyzed by glycerol-3-phosphate acyltransferase. Then, catalysis is performed through lysophosphatidyl acyltransferase to produce phosphatidic acid, which forms diacylglycerol (DAG) in the PAP reaction (Brindley, 1984). DAG is used not only to synthesize TAG, but also in the syntheses of phosphatidylethanolamine and phosphatidylcholine, which are the main constituents of membranes (Carman and Henry, 1999; Sorger and Daum, 2003). Phosphatidic acid through CDP-diacylglycerol by CDP-diacylglycerol synthetase is an alternative pathway to synthesize membrane phospholipids and their derivatives. Moreover, PAPs can regulate phospholipid synthesis at the transcriptional level (Santos-Rosa *et al*., 2005). The production of DAG by PAP to activate protein kinase C is an important signal pathway in response to stress (Exton, 1994; Testerink and Munnik, 2005; Howe and McMaster, 2006). The four PAP homologous genes *PAH1*, *DPP1*, *LPP1*, and *APP1* are responsible for the PAP activity detectable in yeasts. *DPP1* and *LPP1* are involved in lipid signaling; they contain six transmembrane domains and a phosphatase domain. They localize in the vacuoles and Golgi body complexes, and use phosphatidic acid (PA), diacylglycerol pyrophosphate (DGPP), lysophosphatidylcholine (LysoPA), and sphingosine 1-phosphate (S1P) as substrates. *PAH1* encodes the only PAP enzyme that is essential to lipid biosynthesis in *Saccharomyces cerevisiae*. The actin patch protein (App1) interacts with endocytic proteins, and may be involved in vesicular transportation through its PAP activity (Chae *et al*., 2012). In *Arabidopsis*, three of the PAP homologous genes, namely, *AtLPP1* (lipid phosphate phosphatase, LPP), *AtLPP2*, and *AtLPP3*, have been identified. *AtLPP1* encodes a 35-kD protein with a phosphatase domain and six transmembrane domains. It has high protein sequence homology with yeast *DPP1*. After the expression of *AtLPP1* in the *S* double mutant dpp1Δlpp1Δ, *AtLPP1* exhibits DGPP and PA phosphatase activities (Pierrugues *et al*., 2001). Moreover, *AtLPP1* tends to use DGPP as a substrate, whereas *AtLPP2* has no substrate use tendencies. *AtLPP1* is expressed mainly in the leaves and roots of *Arabidopsis*, whereas *AtLPP2* is expressed in all parts. Unlike *AtLPP2*, the gene expression of *AtLPP1* improves when *Arabidopsis* is treated with ionization radiation, ultraviolet-B (UV-B) radiation, or mast cell-degranulating peptides. Thus, we conclude that *AtLPP1* has an important role in the response to abiotic stress.

Merchant *et al.* (2007) predicted three of the PAP-homologous genes in *Chlamydomonas*: *PAP1*, *PAP2*, and *PAH1*. Of the three genes, only *PAP2* has a full-length coding sequence. Thus far, no evidence has demonstrated that *CrPAP2* gene expression and regulation are related to cellular lipid accumulation in *Chlamydomonas*. Accordingly, this study aimed to determine whether such a relationship exists. High levels of mRNA of *CrPAP2* and lipid accumulation were detected in *C. reinhardtii* CC124 in the presence and absence of nitrogen. Suppression by RNAi and over-expression of the *CrPAP2* gene were then performed in *Chlamydomonas* to ascertain whether the over-expression or inhibition of *CrPAP2* affected lipid accumulation.

2 Materials and methods

2.1 Bioinformatics analysis of *PAP2*

Information on the *Chlamydomonas PAP2* gene (JGI Protein ID: 343983) was obtained from the JGI *Chlamydomonas* database. A transmembrane assay was conducted using TMHMM 2.0. Euk-mPLoc 2.0 was used to predict the subcellular localization of proteins (Chou and Shen, 2008; 2010a; 2010b; 2010c; Chou *et al*., 2011; 2012; Wu *et al.*, 2011; Chou, 2013). Sequence alignment and the phylogenetic tree of the *PAP2* were created using MEGA version 4.1 (Tamura *et al.*, 2007). Active consensus sites were identified

based on the Sanger Pfam database (http://pfam.sanger.ac.uk/search).

2.2 Cultivation conditions and biomass analysis of *Chlamydomonas*

Algal strain *C. reinhardtii* CC425 (mt) was used as the receptor strain in a transgenic assay using tris acetate phosphate (TAP) agar plates and high salt medium (HSM) liquid medium for algae cultivation (Harris, 1989; Deng *et al.*, 2011). All algae strains used in this study are listed in Table 1. For HSM-N medium, the components were the same as HSM, except for the replacement of NaCl with NH_4Cl. The cultured cells were stored in an incubator at a light intensity of 150 μmol/(m^2·s) or on a shaker at 230 r/min at 25 °C.

Table 1 Algae strain names used in this study

Name	Strain
C. reinhardtii CC425	cw-15, arg-2
Maa7-4 (10, 19)	pMaa7IR/XIR transgenic algae strains
PAP2-RNAi-3 (10, 56)	*CrPAP2* RNAi transgenic algae strains
pCAMBIA-2 (8, 16)	pCAMBIA1302 transgenic algae strains
pCAMBIA-PAP2-4 (26, 60)	*CrPAP2* over-expression transgenic algae strains

The algal biomass (g/L) of samples was detected at an optical density of 490 nm (OD_{490}), as described in a previous study (Deng *et al.*, 2012). To generate the standard curve of OD_{490} versus biomass (g/L) and guarantee that the OD_{490} values ranged from 0.15 to 0.75, a series of *C. reinhardtii* CC425 samples were collected and diluted to appropriate ratios. The dry cell weights and OD_{490} values of samples were detected. According to the results of the standard curve, the biomass was calculated using the following formula: dry cell weight (g/L)=0.7444×OD_{490}–0.0132 (supplementary Fig. S1).

2.3 Analysis of algal lipid content

To determine the neutral lipid level, a fluorescence method was used in accordance with the description of Deng *et al.* (2011). To generate the standard curve of the neutral lipid content and the fluorescence value, different concentrations of triolein (Sigma, USA) were used to measure fluorescence values after staining with Nile Red. The following formula was used to detect the algal lipid content: lipid content (g/g)=(0.0004×$FD_{470/570}$–0.0038)×0.05/dry cell weight, where $FD_{470/570}$ is the fluorescence value with an excitation wavelength of 470 nm and an emission wavelength of 570 nm (supplementary Fig. S2). For the microscopic assay, samples were stained with 0.1 mg/ml Nile Red. Results were acquired using a fluorescence microscope (Nikon 80i) (Gao *et al.*, 2008; Chen *et al.*, 2009; Huang *et al.*, 2009).

2.4 RNA extraction and cloning of *CrPAP2* gene

The *CrPAP2* gene was amplified by polymerase chain reaction (PCR) using total RNA prepared through a modified method of Li *et al*. (2012). Cells from 10 ml of cultivated algae were collected by centrifugation at 10000×*g* for 1 min. The supernatant was extracted using phenol and chloroform. Total RNA was precipitated with ethanol and dissolved with RNase-free water. For reverse transcription, the cDNA of *C. reinhardtii* CC425 was synthesized and diluted 10 times using the template for amplifying the *CrPAP2* gene. PCR reactions were performed with two primers, namely, PAP2L (5′-ATTTTAGCGTT GTCGCCACT-3′) and PAP2R (5′-AGCAGCCAATT TGGTTTTGT-3′), and templates in a final volume of 50 μl of the reaction system. The resulting DNA fragment was purified using a DNA gel extraction kit (BBI, Canada), and inserted into the cloning vector pMD18-T. The constructs were identified by restriction enzyme digestion and sequencing. The sequenced plasmid was named pMD18T-PAP2.

2.5 Generating RNAi vector against *CrPAP2* gene

To generate the RNAi vector for knockdown of *CrPAP2* gene, we used plasmid pMD18T-PAP2 as a template, as well as primers PAP2RNAiL (5′-GCGTGTTTGCCTACTTCCTC-3′) and PAP2RNAiR (5′-CACTACTCGCGCCGTACAT-3′), to amplify the fragment of *CrPAP2* and its reverse complement sequences. Then, the amplified fragments were digested with *Hin*dIII/*Sal*I and *Kpn*I/*Bam*HI, and cloned into pMD18T-18S to obtain the construct pMD18-CrPAP2F-18S-CrPAP2R, which contained the inverted repeat sequence of *CrPAP2* (*CrPAP2* IR). Finally, *CrPAP2* IR was digested with *Kpn*I and *Hin*dIII, and inserted into pMaa7/XIR to obtain pMaa7IR/*CrPAP2* IR.

2.6 Construction of the over-expression vector of *CrPAP2* gene for *Chlamydomonas*

To construct the over-expression vector of *CrPAP2* gene, the coding sequence of *CrPAP2* was amplified by PCR using pMD18T-PAP2 as a template and primers 5′-TAGTAGATCTGATGGACGCGGTG ACCAC-3′ and 5′-TATAACTAGTTCACCCCGTG TTCTGCATGCC-3′. The fragment was then digested with *Nco*I/*Spe*I and inserted into a similarly-digested pCAMBIA1302 to give pCAMPAP2, which allows over-expression of *CrPAP2*.

2.7 Transformation of *Chlamydomonas*

A modified glass bead method described by Kindle (1990) was used for the transformation of *C. reinhardtii* strain CC425. A single colony of algae was inoculated into 50 ml of TAP medium and cultivated for about 2–3 d to reach a cell density of 2×10^6 cells/ml. These cells were used as recipients for transformation after collection and dilution by TAP. For transformation, sterile glass beads, DNA, recipient cells, and polyethylene glycol were mixed using a vortex. Finally, the mixtures were incubated in TAP plates for 7 d until the transgenic strain appeared in the medium. For over-expression of *PAP2* gene, 50 μg/ml hygromycin TAP medium was used. Knockdown of *PAP2* by RNAi was performed using TAP medium containing 5 μmol/L 5-FI, 5 μg/ml paromomycin, and 1.5 mmol/L L-tryptophan.

2.8 Expression of *CrPAP2* in *Escherichia coli* BL21

To express *CrPAP2* in *E. coli* BL21, the coding region was amplified from pMD18T-PAP2 with the primer pairs GEXPPAP2F (5′-TATGGGATCCAT GGTCAATTGGAATAGT-3′) and GEXPAP2R (5′-TATAGTCGACCTAGTATCGCCCACTGAC-3′). The amplified fragments were digested with *Bam*HI/*Sal*I and inserted into a similarly-digested pGEX-6p-1 to give pGEXPAP2. Transformation of *E. coli* BL21, subsequent foreign protein detection using sodium dodecyl sulfate polyacrylamide gel electrophoresis (SDS-PAGE), and purification of the glutathione *S*-transferase (GST)-fusion protein were performed as described by Sambrook and Russell (2001).

2.9 Quantitative identification of *PAP2* RNA

Real-time PCR was used to analyze the RNA level of *PAP2* gene in HSM or HSM-N conditions, and detect the RNA level of *PAP2* in RNAi and the over-expressed transgenic line. RNA samples were prepared using TRIzol, as described by Fei and Deng (2007). After cDNA was synthesized and used as a template, real-time PCR was performed on a BioRad iCycler using the *PAP2* gene-specific primers PAP2RNAiL (5′-GCGTGTTTGCCTACTTCCTC-3′) and PAP2RNAiR (5′-CACTACTCGCGCCGTAC AT-3′) to calculate the quantity of *PAP2* RNA. SYBR Green was used as the fluorescent dye. The 18S rRNA of *Chlamydomonas* was used as an internal control with primers 5′-CCGTGTCAGGATTGGGTAAT TT-3′ and 5′-TCAACTTTCGATGGTAGGATAG TG-3′. All reactions were performed three times. We calculated the amplification rate using a baseline-subtraction method. Relative differences in RNA were evaluated using the $2^{-\Delta\Delta C_T}$ method, as described by Livak and Schmittgen (2001).

2.10 Measurement of PAP activities

The method of Ullah *et al.* (2012) was used to measure the *CrPAP2* activities. The amount of Pi in nmoles released by PAP from the substrate dioleoylphosphatidate (1,2-dioleoyl-*sn*-glycero-3-phosphate, sodium salt) was determined. The reaction was stopped by the addition of 2 ml AMA reagent (acetone: 10 mmol/L ammonium molybdate:5 mol/L sulfuric acid mixture, 2:1:1 (v/v/v)), followed by 100 ml of 1 mol/L citrate solution. The resulting turbidity was removed using centrifugation at 12 000×*g* for 6 min at room temperature. The absorbance of the resulting yellow color was read at 355 nm using a spectrophotometer. The enzyme unit, kat, was defined as the moles of the substrate converted per second (Heinonen and Lahti, 1981; Ullah *et al.*, 2005).

3 Results

3.1 Cloning of *CrPAP2* gene and bioinformatics analysis

The gene sequence of *PAP2* listed in the JGI database (JGI Protein ID: 343983) was used for the design of primers for the amplification of the gene. A full-length *CrPAP2* gene was amplified by PCR. A DNA fragment of about 1 000 bp was inserted into the pMD-18T vector and sequenced. Compared with the 343983 sequence in the JGI *C. reinhardtii* v4.0

database, the cloned *CrPAP2* CDS had a sequence with 978 bp and showed 100% consistency. This cloned fragment was named *CrPAP2*.

We constructed a phylogenetic tree of the members of the lipid phosphate phosphatase protein family, including *C. reinhardtii CrPAP2* and *Arabidopsis* AtLpp1p, AtLpp2p, and AtLpp3p proteins (Fig. 1). *C. reinhardtii CrPAP2* was grouped with the putative *Caenorhabditis elegans* phosphate phosphatase protein Q19403 in one branch, whereas *Arabidopsis* AtLpp1p, AtLpp2p, and AtLpp3p proteins and *S. cerevisiae* Dpp1p and Lpp1p proteins were grouped in a main branch (Fig. 1). Analyses indicated that *C. reinhardtii CrPAP2* was a lipid phosphate phosphatase enzyme. Moreover, the location of *CrPAP2* was predicted by Euk-mPLoc 2.0 to be in the membrane because *CrPAP2* has five transmembrane helices (TMHMM result). As TAG can be synthesized in the endoplasmic reticulum (ER) and in the chloroplasts of *Chlamydomonas*, the possible location of *CrPAP2* is in the membranes of ER or chloroplasts (Liu and Benning, 2013).

3.2 mRNA level of *CrPAP2* under N-sufficient and N-limited conditions

To determine the mRNA levels of CrPEPC1-1, we collected cells of *Chlamydomonas* (2×10^6 cells/ml) by centrifugation. After washing, the cells were transferred to the HSM or HSM-N medium for further cultivation. The algal cells that were harvested at 24, 48, 72, or 96 h were used for RNA extraction. We quantitatively determined the expression of *CrPAP2*

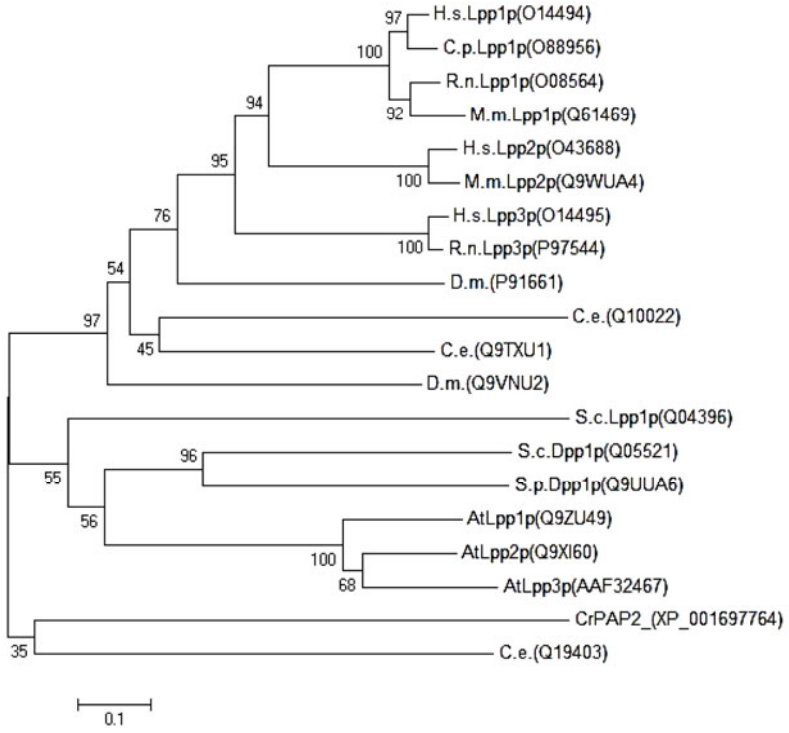

Fig. 1 Phylogenetic analysis of the lipid phosphate phosphatase protein family

C. reinhardtii CrPAP2, *Arabidopsis* AtLpp1p, AtLpp2p, and AtLpp3p proteins, *S. cerevisiae* Dpp1p and Lpp1p proteins, all available mammalian lipid phosphate phosphatase proteins, *Drosophila* Wunen protein, as well as uncharacterized putative lipid phosphate phosphatase-like proteins identified in *A. thaliana*, *D. melanogaster*, *C. elegans*, and *Schizosaccharomyces pombe* genomes, were used for comparison. The tree was built using the neighbor joining method, wherein point accepted mutation (PAM) distances were computed based on reliably aligned sites. The SwissProt accession numbers (in brackets) designate all protein sequences. The length of horizontal branches is such that the evolutionary distance between two proteins is proportional to the total length of the horizontal branches that connect them. Bootstrap values are shown at the nodes. H.s. Lpp1p, Lpp2p, and Lpp3p: *Homo sapiens* Lpp1p, Lpp2p, and Lpp3p; S.c.Dpp1p: *Saccharomyce scerevisiae* Dpp1p; S.p.Dpp1p: *Schizosaccharomyces pombe* Dpp1p; R.n. Lpp1p and Lpp3p: *Rattus norvegicus* Lpp1p and Lpp3p; M.m. Lpp1p and Lpp2p: *Mus musculus* Lpp1p and Lpp2p; D.m.: *D. melanogaster* lipid phosphate phosphatase; C.e.: *C. elegans* lipid phosphate phosphatase; C.p.Lpp1p: *Cavia porcellus* Lpp1p

gene in these samples using reverse transcription and real-time PCR. Results indicate that the cells accumulated 2–5 times more lipid under the −N condition than the +N condition (Fig. 2). In addition, the mRNA levels of *CrPAP2* increased significantly. Thus, we investigated whether the increase in the level of mRNA of *CrPAP2* influenced lipid accumulation.

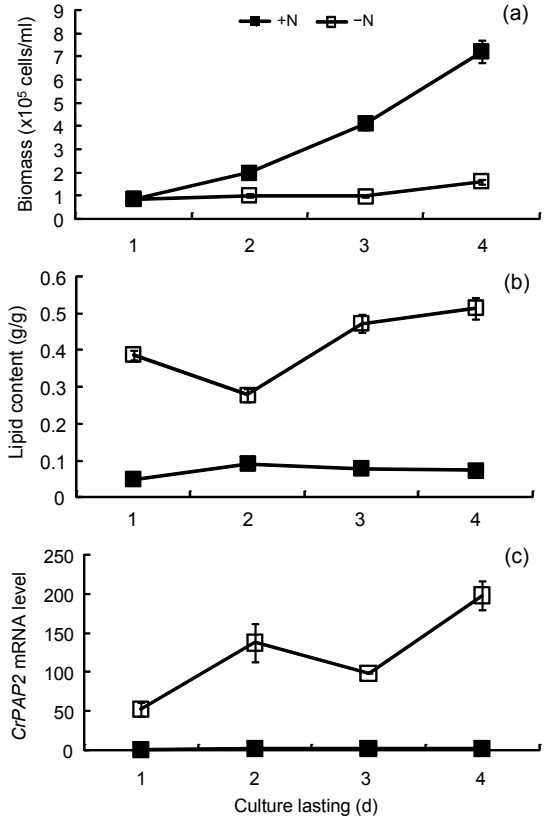

Fig. 2 Biomass (a), lipid content (b), and mRNA levels (c) of *CrPAP2* in HSM and HSM-N medium
The mRNA levels of *C. reinhardtii* CC425 samples grown in the indicated medium for 1, 2, 3, or 4 d, were analyzed using RT-PCR. +N: cells cultivated in N-sufficient HSM medium; −N: cells cultivated in N-free HSM medium. Data are expressed as mean±SD (n=3)

3.3 Silencing of *CrPAP2* decreased lipid content in *C. reinhardtii*

To determine further the relationship between *CrPAP2* expression and lipid accumulation, we examined the effects of artificial silencing of the *CrPAP2* gene on the lipid content of *C. reinhardtii*. Based on the *CrPAP2* (343983) sequences retrieved from the JGI *C. reinhardtii* v4.0 database, we designed primers to amplify the fragment of the coding region of *CrPAP2*. The DNA fragment was subcloned and then used to generate the *CrPAP2* RNAi construct pMaa7IR/*CrPAP2* IR. After transforming the silencing construct into *C. reinhardtii* CC425, more than 150 positive transformants were obtained. We selected three transgenic algae for measuring the lipid content and mRNA levels of the target gene. Strains transformed with the vector pMaa7IR/XIR were used as controls. Analysis of the transgenic algae revealed that the lipid content decreased by 12.4%–17.4% after 6 d of cultivation (Fig. 3b), although no differences in their growth were found (Fig. 3a). To evaluate the effectiveness of our RNAi constructs, we analyzed the abundance of target gene-specific mRNA using real-time PCR in transgenic algae. The level of the mRNA of *CrPAP2* decreased to 83.4% from 94.0% (Fig. 3c), indicating high-efficiency silencing by these constructs.

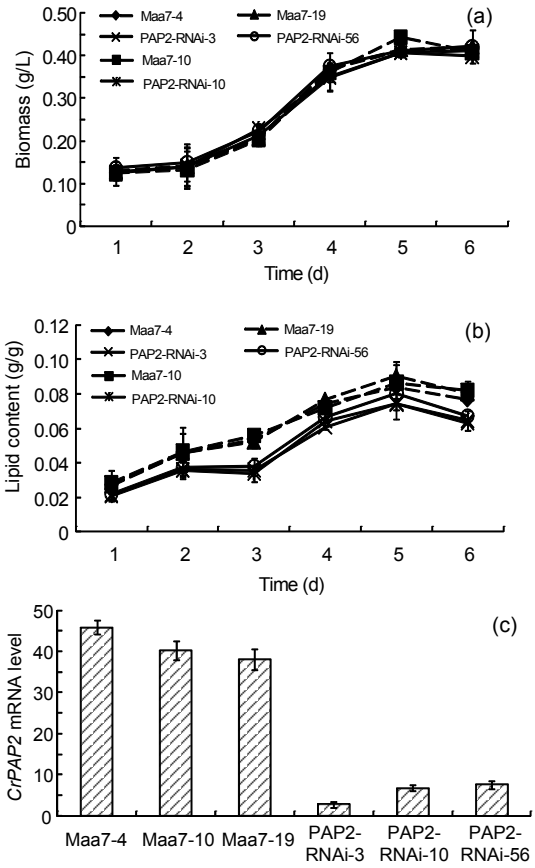

Fig. 3 Biomass (a), lipid content (b), and mRNA levels (c) of *CrPAP2* RNAi transgenic algae strains
Maa7-4 (10, 19), pMaa7IR/XIR transgenic algae strains; PAP2-RNAi-3 (10, 56), pMaa7IR/*CrPAP2* IR transgenic algae strains. Data are expressed as mean±SD (n=3)

Similar results were obtained from Nile Red staining. Based on microscopic analysis, fewer oil droplets with yellow fluorescence were found in *CrPAP2* RNAi transgenic algae than in the pMaa7IR/XIR transgenic algae (Fig. 4). These data indicate that the regulation of *CrPAP2* gene expression can affect the cell lipid content.

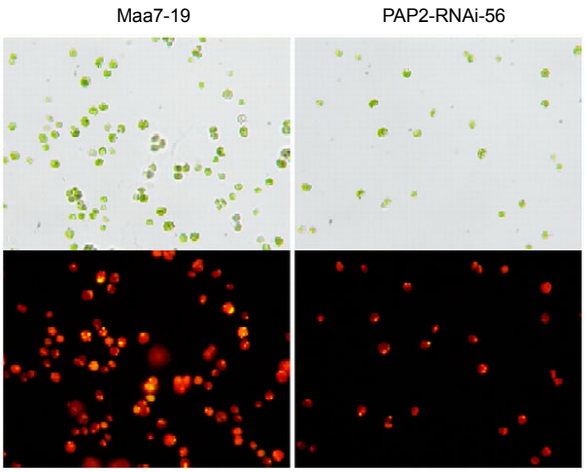

Fig. 4 Microscopic observation of *CrPAP2* transgenic algae strains (250× Nikio 80i)

Above: bright field, for cell morphology; Below: dark field, for oil droplets. After 4 d of cultivation in HSM medium, fewer oil droplets of *CrPAP2* RNAi transgenic algae were found. Maa7-19, pMaa7IR/XIR transgenic algae strain number 19; PAP2-RNAi-56, pMaa7IR/*CrPAP2* IR transgenic algae strain number 56

3.4 Over-expression of *CrPAP2* improved lipid content in *C. reinhardtii*

The decrease in lipid content caused by RNAi silencing of *CrPAP2* suggested that the expression of the *CrPAP2* gene affected the biosynthesis of triglycerides in *C. reinhardtii*. Thus, we examined whether *CrPAP2* over-expression could increase the lipid content in *C. reinhardtii*. The pCAMPAP2 vectors that expressed the *CrPAP2* gene from the CAMV 35S promoter were introduced into *C. reinhardtii*. The lipid contents and growth rates of three randomly selected transgenic algae were determined in each transgenic algae line. Over-expression of the *CrPAP2* gene increased growth rate in the early stages from Days 2 to 5 (Fig. 5a). Compared with the control pCAMBIA1302 transgenic algae lines, the over-expression of *CrPAP2* increased lipid content. For instance, after 6 d of growth in HSM medium, the lipid contents of transgenic algae increased by 7.5%–21.8% (Fig. 5b). Compared with pCAMBIA1302 transgenic stains, the mRNA levels of *CrPAP2* increased by 329%–523% (Fig. 5c). Moreover, analysis of the PAP activities of

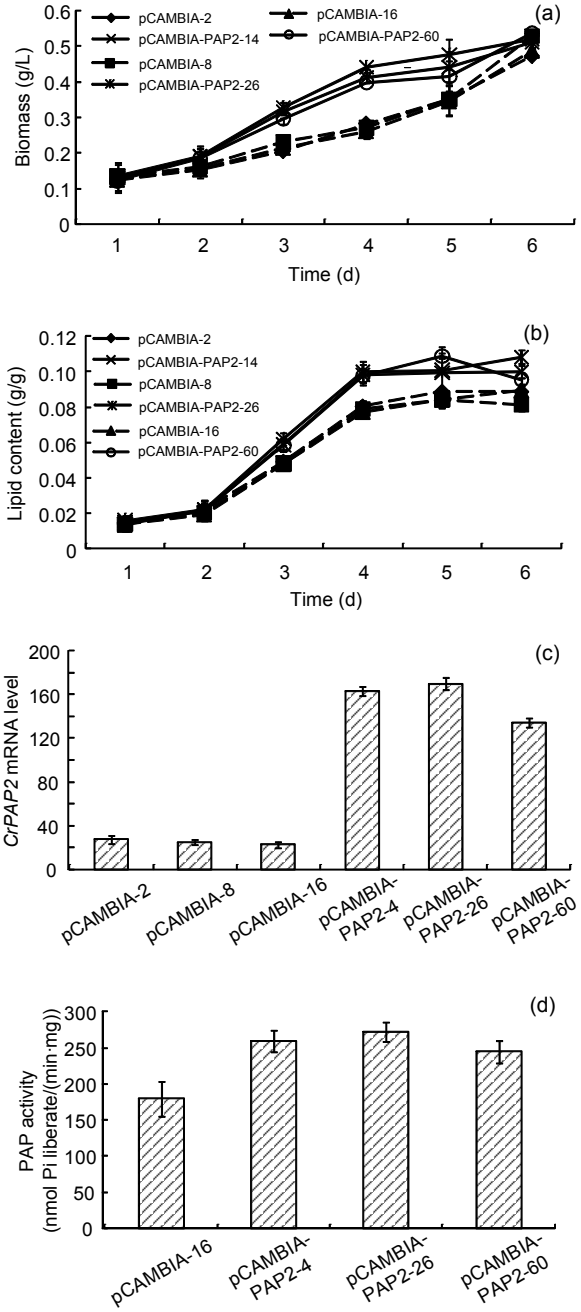

Fig. 5 Biomass (a), lipid content (b), mRNA level (c), and PAP activity (d) assays of *CrPAP2* over-expression transgenic algae in HSM medium

pCAMBIA-2 (8, 16), pCAMBIA1302 transgenic algae strains; pCAMBIA-PAP2-4 (26, 60), pCAMPAP2 transgenic algae strains. Data are expressed as mean±SD (n=3)

the transgenic lines showed a modest increase in PAP activity (Fig. 5d). The increase in lipid content was also observed using Nile Red dye staining (Fig. 6). More oil droplets were found in *CrPAP2* over-expression transgenic algae compared with the controls, as determined by microscopic analysis. These data indicate that an increase in *CrPAP2* gene expression improved cell lipid content.

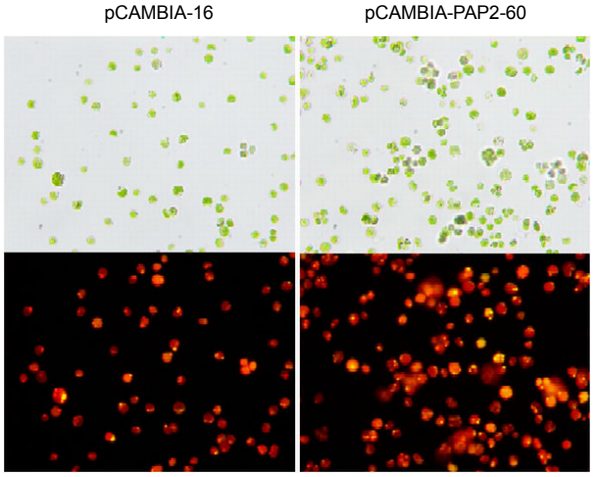

Fig. 6 Lipid content in a transgenic algae line detected by Nile Red staining (250× Nikio 80i)
Above: bright field, for cell morphology; Below: dark field, for oil droplets. After 4 d of cultivation in HSM medium, more oil droplets of *CrPAP2* transgenic algae were found. pCAMBIA-16, pMCAMBIA1302 transgenic algae strain number 16; pCAMBIA-PAP2-60, pCAMPAP2 transgenic algae strain number 60

3.5 Expression of CrPAP2 in *E. coli* BL21 and detection of in vitro enzyme activity

The plasmid pGEX-6p-1-PAP2 was constructed to express *CrPAP2* genes in *E. coli* to verify their enzyme activities. The recombinant vector was transformed into the *E. coli* BL21 strain. Transformants were grown in lysogeny broth medium and induced with 1 mmol/L of isopropylthiogalactoside. The supernatant was then loaded onto a 15% SDS-PAGE gel. A GST-CrPAP2 protein band of 60 kD was observed (Fig. 7a). The fusion proteins were purified using columns, followed by enzyme activity assay (Figs. 7b and 7c). Compared with the control, the enzyme activity of *CrPAP* increased by 27- to 29-fold (Fig. 7c). This behavior indicated that the cloned *CrPAP2* gene exhibits biological activities.

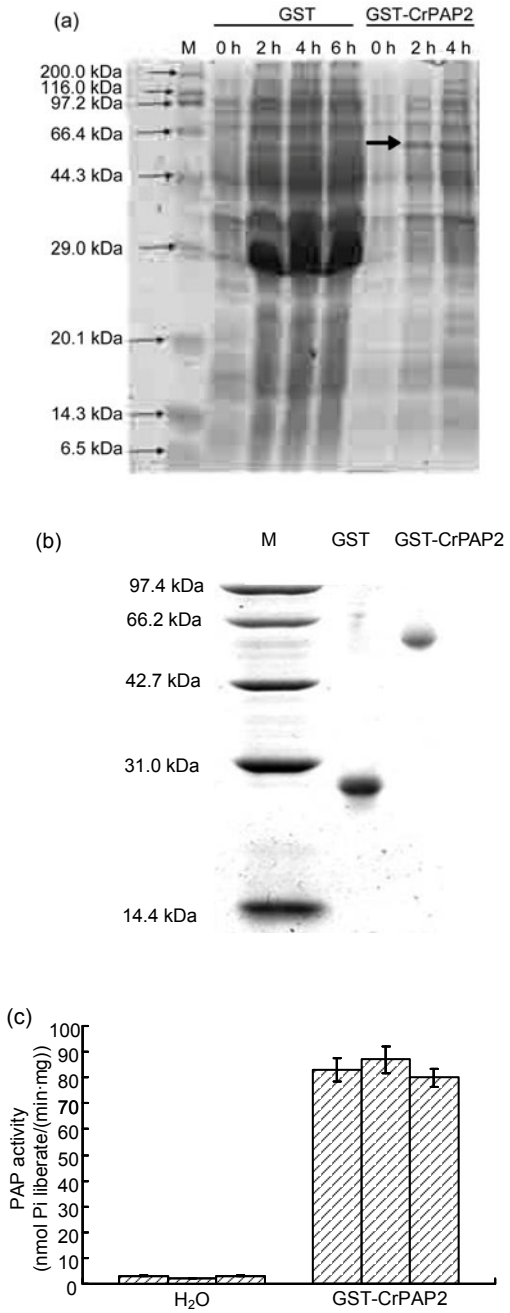

Fig. 7 Expression of CrPAP2 in *E. coli* BL21 and in vitro enzyme activity assay
After induction by IPTG and cultivation for 0, 2, or 4 h, total protein was harvested and run on SDS-PAGE. (a) Expression of CrPAP2 in *E. coli* BL21; (b) The purified GST-CrPAP2; (c) In vitro enzyme activity assay of GST-CrPAP2. GST, *E. coli* BL21 transformed with pGEX-6p-1; GST-CrPAP2, *E. coli* BL21 transformed with plasmid pGEX-6p-1-PAP2 to express the fusion protein GST-CrPAP2. The induction time of the cultured cells is indicated by 0, 2, 4, and 6 h. The GST and GST-CrPAP2 fusion proteins are indicated by the arrow

4 Discussion

PAP is a very important enzyme in lipid biosynthesis. This enzyme cleaves the phosphomonoester bond present in PA, yielding DAG and Pi (Smith *et al.*, 1957; Carman, 1997). PAP acts as a pivotal biocatalyst in the metabolic flux between the different classes of glycerolipids within the endoplasmic reticulum and has an important role in the phospholipase D signaling pathway (Exton, 1994). Several PAP enzymes have been described from *S. cerevisiae*, mammalian, and *Arabidopsis* cells (Phan and Reue, 2005; Hans *et al.*, 2006). These enzymes can utilize a variety of lipid phosphate substrates in vitro, including lysophosphatidic acid, phosphatidic acid, diacylglycerol pyrophosphate, sphingosine 1-phosphate, and ceramide 1-phosphate, to form DAG. They are important in lipid accumulation and cell signal transductions. In the Kennedy pathway of TAG synthesis, formation of DAG is the integral step. Moreover, DAG is not only essential for TAG formation, but is also a substrate in the synthesis of phosphatidylethanolamine (PE) and phosphatidylcholine (PC). In *Chlamydomonas*, instead of PC, the betaine lipid diacylglyceryl-*N*,*N*,*N*-trimethylhomoserine (DGTS) is the predominant glycerolipid building block of membranes (Klug and Benning, 2001). Therefore, the up- or down-regulation of PAP activities affects the content of DAG, which also affects the content of TAG, PE, and DGTS. In this study, we identified a new *Chlamydomonas* phosphate phosphatase gene, *CrPAP2*, which is different from genes in the mammalian or *Arabidopsis* phosphate phosphatase gene families. The in vitro expression protein has the same function as phosphate phosphatase, namely, it catalyzes the reaction of phosphatidic acid to yield diacylglycerol and Pi. We showed that an increase or decline in the expression of the gene could affect the lipid content of algal cells. Our findings suggest that increasing oil content can result from the over-expression of *CrPAP2* in microalgae. Further research on CDP-ethanolamine:diacylglycerol ethanolamine phosphotransferases and betaine lipid synthase will help in understanding TAG metabolism and phospholipid biosynthesis in photosynthetic eukaryotic cells.

Compliance with ethics guidelines

Xiao-dong DENG, Jia-jia CAI, and Xiao-wen FEI declare that they have no conflict of interest.

This article does not contain any studies with human or animal subjects performed by any of the authors.

References

Brindley, D.N., 1984. Intracellular translocation of phosphatidate phosphohydrolase and its possible role in the control of glycerolipid synthesis. *Prog. Lipid Res.*, **23**(3): 115-133. [doi:10.1016/0163-7827(84)90001-8]

Brindley, D.N., 2004. Lipid phosphate phosphatases and related proteins: signaling functions in development, cell division, and cancer. *J. Cell Biochem.*, **92**(5):900-912. [doi:10.1002/jcb.20126]

Carman, G.M., 1997. Phosphatidate phosphatases and diacylglycerol pyrophosphate phosphatases in *Saccharomyces cerevisiae* and *Escherichia coli*. *BBA-Lipid. Lipid Metab.*, **1348**(1-2):45-55. [doi:10.1016/S0005-2760(97)00095-7]

Carman, G.M., Henry, S.A., 1999. Phospholipid biosynthesis in the yeast *Saccharomyces cerevisiae* and interrelationship with other metabolic processes. *Prog. Lipid Res.*, **38**(5-6):361-399. [doi:10.1016/S0163-7827(99)00010-7]

Chae, M., Han, G.S., Carman, G.M., 2012. The *Saccharomyces cerevisiae* actin patch protein App1p is a phosphatidate phosphatase enzyme. *J. Biol. Chem.*, **287**(48):40186-40196. [doi:10.1074/jbc.M112.421776]

Chen, W., Zhang, C., Song, L., Sommerfeld, M., Hu, Q., 2009. A high throughput Nile red method for quantitative measurement of neutral lipids in microalgae. *J. Microbiol. Meth.*, **77**(1):41-47. [doi:10.1016/j.mimet.2009.01.001]

Chou, K.C., 2013. Some remarks on predicting multi-label attributes in molecular biosystems. *Mol. Biosyst.*, **9**(6): 1092-1100. [doi:10.1039/c3mb25555g]

Chou, K.C., Shen, H.B., 2008. Cell-PLoc: a package of Web servers for predicting subcellular localization of proteins in various organisms. *Nat. Protoc.*, **3**(2):153-162. [doi:10.1038/nprot.2007.494]

Chou, K.C., Shen, H.B., 2010a. A new method for predicting the subcellular localization of eukaryotic proteins with both single and multiple sites: Euk-mPLoc 2.0. *PLoS ONE*, **5**(4):e9931. [doi:10.1371/journal.pone.0009931]

Chou, K.C., Shen, H.B., 2010b. Cell-PLoc 2.0: an improved package of web-servers for predicting subcellular localization of proteins in various organisms. *Nat. Sci.*, **2**(10): 1090-1103. [doi:10.4236/ns.2010.210136]

Chou, K.C., Shen, H.B., 2010c. Plant-mPLoc: a top-down strategy to augment the power for predicting plant protein subcellular localization. *PLoS ONE*, **5**(6):e11335. [doi:10.1371/journal.pone.0011335]

Chou, K.C., Wu, Z.C., Xiao, X., 2011. iLoc-Euk: a multi-label classifier for predicting the subcellular localization of singleplex and multiplex eukaryotic proteins. *PLoS ONE*, **6**(3):e18258. [doi:10.1371/journal.pone.0018258]

Chou, K.C., Wu, Z.C., Xiao, X., 2012. iLoc-Hum: using accumulation-label scale to predict subcellular locations of human proteins with both single and multiple sites. *Mol. Biosyst.*, **8**(2):629-641. [doi:10.1039/c1mb05420a]

Deng, X.D., Li, Y.J., Fei, X.W., 2011. The mRNA abundance of *pepc2* gene is negatively correlated with oil content in *Chlamydomonas reinhardtii*. *Biomass Bioenerg.*, **35**(3): 1811-1817. [doi:10.1016/j.biombioe.2011.01.005]

Deng, X.D., Gu, B., Li, Y.J., Hu, X.W., Guo, J.C., Fei, X.W., 2012. The roles of acyl-CoA: diacylglycerol acyltransferase 2 genes in the biosynthesis of triacylglycerols by the green algae *Chlamydomonas reinhardtii*. *Mol. Plant*, **5**(4): 945-947. [doi:10.1093/mp/sss040]

Exton, J.H., 1994. Phosphatidylcholine breakdown and signal transduction. *BBA-Lipid. Lipid Metab.*, **1212**(1):26-42. [doi:10.1016/0005-2760(94)90186-4]

Fei, X.W., Deng, X.D., 2007. A novel Fe deficiency responsive element (FeRE) regulates the expression of *atx1* in *Chlamydomonas reinharditii*. *Plant Cell Physiol.*, **48**(10): 1496-1503. [doi:10.1093/pcp/pcm110]

Gao, C.F., Xiong, W., Zhang, Y.L., Yuan, W.Q., Wu, Q.Y., 2008. Rapid quantitation of lipid in microalgae by time-domain nuclear magnetic resonace. *J. Microbiol. Meth.*, **75**(3):437-440. [doi:10.1016/j.mimet.2008.07.019]

Hans, G.S., Wu, W.I., Carman, G.M., 2006. The *Saccharomyces cerevisiae* lipin homolog is a Mg^{2+}-dependent phosphatidate phosphatase enzyme. *J. Biol. Chem.*, **281**: 9210-9218. [doi:10.1074/jbc.M600425200]

Harris, E.H., 1989. The *Chlamydomonas* Source Book: A Comprehensive Guide to Biology and Laboratory Use. Academic Press, San Diego, CA.

Heinonen, J.K., Lahti, R.J., 1981. A new and convenient colorimetric determination of inorganic orthophosphate and its application to the assay of inorganic pyrophosphatase. *Anal. Biochem.*, **113**(2):313-317. [doi:10.1016/0003-2697(81)90082-8]

Howe, A.G., McMaster, C.R., 2006. Regulation of phosphatidylcholine homeostasis by Sec14. *Can. J. Physiol. Pharm.*, **84**(1):29-38. [doi:10.1139/Y05-138]

Huang, G.H., Chen, G., Chen, F., 2009. Rapid screening method for lipid production in alga based on Nile red fluorescence. *Biomass Bioenerg.*, **33**(10):1386-1392. [doi:10.1016/j.biombioe.2009.05.022]

Kindle, K.L., 1990. High frequency nuclear transformation of *Chlamydomonas reinhardtii*. *PNAS*, **87**(3):1228-1232. [doi:10.1073/pnas.87.3.1228]

Klug, R.M., Benning, C., 2001. Two enzymes of diacylglyceryl-*O*-4′-(*N*,*N*,*N*,-trimethyl) homoserine biosynthesis are encoded by *btaA* and *btaB* in the purple bacterium *Rhodobacter sphaeroides*. *PNAS*, **98**(10):5910-5915. [doi:10.1073/pnas.101037998]

Li, Y.J., Fei, X.W., Deng, X.D., 2012. Novel molecular insights into nitrogen starvation-induced triacylglycerols accumulation revealed by differential gene expression analysis in green algae *Micractinium pusillum*. *Biomass Bioenerg.*, **42**:199-211. [doi:10.1016/j.biombioe.2012.03.010]

Liu, B., Benning, C., 2013. Lipid metabolism in microalgae distinguishes itself. *Curr. Opin. Biotech.*, **24**(2):300-309. [doi:10.1016/j.copbio.2012.08.008]

Livak, K.J., Schmittgen, T.D., 2001. Analysis of relative gene expression data using real-time quantitative PCR and the $2^{-\Delta\Delta C_T}$ method. *Methods*, **25**(4):402-408. [doi:10.1006/meth.2001.1262]

Merchant, S.S., Prochnik, S.E., Vallon, O., Harris, E.H., Karpowicz, S.J., Witman, G.B., Terry, A., Salamov, A., Fritz-Laylin, L.K., Maréchal-Drouard, L., *et al*., 2007. The *Chlamydomonas* genome reveals the evolution of key animal and plant functions. *Science*, **318**(5848): 245-250. [doi:10.1126/science.1143609]

Nanjundan, M., Possmayer, F., 2003. Pulmonary phosphatidic acid phosphatase and lipid phosphate phosphohydrolase. *Am. J. Physiol. Lung Cell Mol. Physiol.*, **284**:L1-L23. [doi:10.1152/ajpcell.00460.2002]

Phan, J., Reue, K., 2005. Lipin, a lypodystrophy and obesity gene. *Cell Metab.*, **1**(1):73-83. [doi:10.1016/j.cmet.2004.12.002]

Pierrugues, O., Brutesco, C., Oshiro, J., Gouy, M., Deveaux, Y., Carman, G.M., Thuriaux, P., Kazmaier, M., 2001. Lipid phosphate phosphatases in *Arabidopsis* regulation of the *AtLPP1* gene in response to stress. *J. Biol. Chem.*, **276**(23):20300-20308. [doi:10.1074/jbc.M009726200]

Sambrook, J., Russell, D.W., 2001. Molecular Cloning: a Laboratory Manual (3-Volume Set). Cold Spring Harbour Laboratory Press, Cold Spring Harbour, New York.

Santos-Rosa, H., Leung, J., Grimsey, N., Peak-Chew, S., Siniossoglou, S., 2005. The yeast lipin Smp2 couples phospholipid biosynthesis to nuclear membrane growth. *EMBO J.*, **24**(11):1931-1941. [doi:10.1038/sj.emboj.7600672]

Sciorra, V.A., Morris, A.J., 2002. Roles for lipid phosphate phosphatases in regulation of cellular signaling. *BBA-Mol. Cell Biol. Lipids*, **1582**(1-3):45-51. [doi:10.1016/S1388-1981(02)00136-1]

Smith, S.W., Weiss, S.B., Kennedy, E.P., 1957. The enzymatic dephosphorylation of phosphatidic acids. *J. Biol. Chem.*, **228**:915-922.

Sorger, D., Daum, G., 2003. Triacylglycerol biosynthesis in yeast. *Appl. Microbiol. Biotechnol.*, **61**:289-299.

Tamura, K., Dudley, J., Nei, M., Kumar, S., 2007. $MEGA_4$: molecular evolutionary genetics analysis (MEGA) software version 4.0. *Mol. Biol. Evol.*, **24**(8):1596-1599. [doi:10.1093/molbev/msm092]

Testerink, C., Munnik, T., 2005. Phosphatidic acid: a multifunctional stress signaling lipid in plants. *Trends Plant*

Sci., **10**(8):368-375. [doi:10.1016/j.tplants.2005.06.002]

Ullah, A.H.J., Sethumadhavan, K., Mullaney, E.J., 2005. Monitoring of unfolding and refolding in fungal phytase (phyA) by dynamic light scattering. *Biochem. Biophys. Res. Commun.*, **327**(4):993-998. [doi:10.1016/j.bbrc.2004.12.111]

Ullah, A.H.J., Sethumadhavan, K., Shockey, J., 2012. Measuring phosphatidic acid phosphohydrolase (EC 3.1.3.4) activity using two phosphomolybdate-based colorimetric methods. *Adv. Biol. Chem.*, **2**(4):416-421. [doi:10.4236/abc.2012.24052]

Wu, Z.C., Xiao, X., Chou, K.C., 2011. iLoc-Plant: a multi-label classifier for predicting the subcellular localization of plant proteins with both single and multiple sites. *Mol. BioSyst.*, **7**:3287-3297. [doi:10.1039/C1MB05232B]

List of electronic supplementary materials

Fig. S1 Correlation between biomass (cell dry weight g/L) and the optical density OD_{490}

Fig. S2 Correlation between lipid concentration (triolein mg/20 ml) and the fluorescence value $FD_{470/570}$